European Geosciences Union General Assembly 2015, EGU

Division Energy, Resources & Environment, ERE

A Diagram of wind speed versus air-sea temperature difference to understand the marine atmospheric boundary layer

Anthony James Kettle*

Geophysical Institute, University of Bergen, Bergen 5020, Norway

Abstract

This contribution reviews the dynamics in the marine atmospheric boundary layer (MABL) with a diagnostic diagram: wind speed versus air-sea temperature difference or U-ΔT. The diagram was first used by Alfred Woodcock in a series of observational studies from the early 1940s of gull flight patterns, and it was revisited in later decades to illustrate the dynamic and thermodynamic controls of fog formation, mesoscale convective clouds, surface fluxes of heat and momentum, whitecap formation, and vessel icing. The present report uses the figure to compare recent met-ocean conditions for a series of Norwegian offshore production platforms in northern Europe.

Keywords: atmospheric stability; Monin-Obukhov length; whitecap; superstructure icing; boundary layer; Woodcock diagram; herring gull

1. Introduction

The rapid development of the offshore wind energy in northwest Europe has focused attention on the typical and extreme met-ocean conditions that can be expected in the near offshore environment where the wind turbines are being constructed. There are important advantages in locating turbines in these offshore areas, including higher

* Corresponding author. Tel.: +47-55583259; fax: +47-55589883.
  E-mail address: ake043@gfi.uib.no

boundary layer wind speeds compared with onshore sites and also the reduced costs of being able to locate an energy plant close to the major market sites in coastal cities [1,2]. On the other hand, it comes with the problems associated with reduced access for maintenance and repair. As well, different dynamical properties in the marine atmospheric boundary layer (MABL) pose challenges for long-term wind turbine operation. Offshore wind turbines are intended to generate power economically over long periods of ~25 years. The offshore technology is still developing but the engineering challenges have mostly focused on firstly designing turbines that can operate without maintenance for long time periods and secondly designing a structure that can withstand bad ocean storms. The economics of the first issue is associated with reducing maintenance costs. This includes a number of normal met-ocean operating issues, but sea salt corrosion and turbulence-related component fatigue have been highlighted as important problems. Lightning damage is a fairly frequent occurrence that may lead to other operational problems [3]. The challenge of designing a structure that can survive bad storms involves making an assessment of the worst wave and wind gusts that a structure will probably experience during an extended time period. The autumn and winter storms in the North Sea are bad, and offshore wind turbines are being located at coastal water depths of 10-100m where unexpected nonlinear ocean dynamical properties may give rise to rogue waves. The international design standard for offshore wind turbines – IEC 61400-3 – summarizes expected met-ocean conditions for ambient turbulence and extreme conditions [4].

The dynamics of the surface wave field and the atmospheric boundary layer is complicated because of the interplay of a number of factors. These include wind speed, air temperature, sea surface temperature, and wind direction. Fetch (i.e., distance upwind to the nearest coastline) also becomes important in assessing the duration of development of the wind wave field. For boundary layer dynamics and wind turbine loading, it is important to simplify the geophysical problem with data projections and diagnostics. For offshore wind energy, the joint-probability distribution described by a data distribution on axes of wind speed versus air minus sea temperature (or the U-ΔT diagram) is important. Boundary layer turbulence depends firstly on wind speed, but it also depends on atmospheric static stability so that the air-sea temperature difference is also significant. This contribution briefly reviews the history of the U-ΔT diagram and presents a number of case studies related to the Norwegian offshore petroleum platforms in the North Seas and Norwegian Sea.

2. Previous Applications of the U-ΔT Diagram

Many problems in data interpretation in marine atmospheric boundary layer research are simplified with the U-ΔT diagram: fog formation and dissipation, cloud formation, turbulent heat flux, whitecap formation, atmospheric pollution dissipation, and superstructure icing. The concept of using wind speed and air-sea temperature difference to explain boundary layer processes developed through 20th century.

2.1. Fog formation

Taylor (1914, 1917) [5,6] used measurements wind speed and air-sea temperature difference to explain fog occurrence during a late winter cruise of the SS *Scotia* to the Grand Banks of Newfoundland and the Labrador Sea. The cruise had been commissioned by the British government in the aftermath of the *Titanic* sinking to understand the meteorological basis of fog formation and iceberg movement that had contributed to the disaster. A series of met-ocean measurements were made at intervals of four hours during the *Scotia* cruise, and Taylor analyzed data to understand fog frequency trends. Taylor's report did not present a U-ΔT diagram but showed summary statistical tables that linked fog frequency with air-sea temperature difference as the main controlling factor. The original data from the *Scotia* cruise report has been reanalyzed in Fig.1a to illustrate that the presence of fog over the sea is mainly a feature of the stable atmospheric boundary layer near the critical Richardson number. In addition to the study of met-ocean conditions of fog formation and dissipation, Taylor also made kite soundings to investigate the evolution of the vertical structure of atmospheric boundary layer as it propagated from the eastern coast of North America out over the Atlantic Ocean [7]. These evolving internal boundary layers propagate from shorelines [8] and complicate the interpretation of MABL conditions with the U-ΔT diagram in coastal areas. Internal boundary

layers have been identified in the high meteorological masts in the North Sea and Baltic Sea that are used to support offshore wind energy development [9,10,11].

2.2. The Woodcock Diagram and Gull Flight Patterns

Alfred Woodcock used the U-ΔT diagram in a series of papers from the 1940s to explain the observed flight characteristics of herring gulls in western North Atlantic Ocean [12,13,14]. In the first publications, the geophysical application of bird flight patterns to understand boundary the layer dynamics was emphasized. At the time, there were no other measurement techniques to assess the temperature and wind structure of the marine atmospheric boundary layer remotely. The seagull flight pattern data set was plotted on a U-ΔT diagram and used to highlight unresolved issues of the structure of convective cells for different regimes of wind speed and atmospheric stability. Replotted in Fig.1b, the Woodcock (1942) [13] diagram indicates simple cell convection patterns at low wind speeds, which evolve into elongated roll vortices at higher wind speed. Lines on the diagram delimit the approximate ranges of the gull flight patterns. These correspond approximately to geophysical stability regions that would later be identified with Richardson number [15] or Monin-Obukhov length scales [16]. The seagull U-ΔT diagrams were an intuitive way to show the dynamics of the boundary layer at a time when offshore meteorological
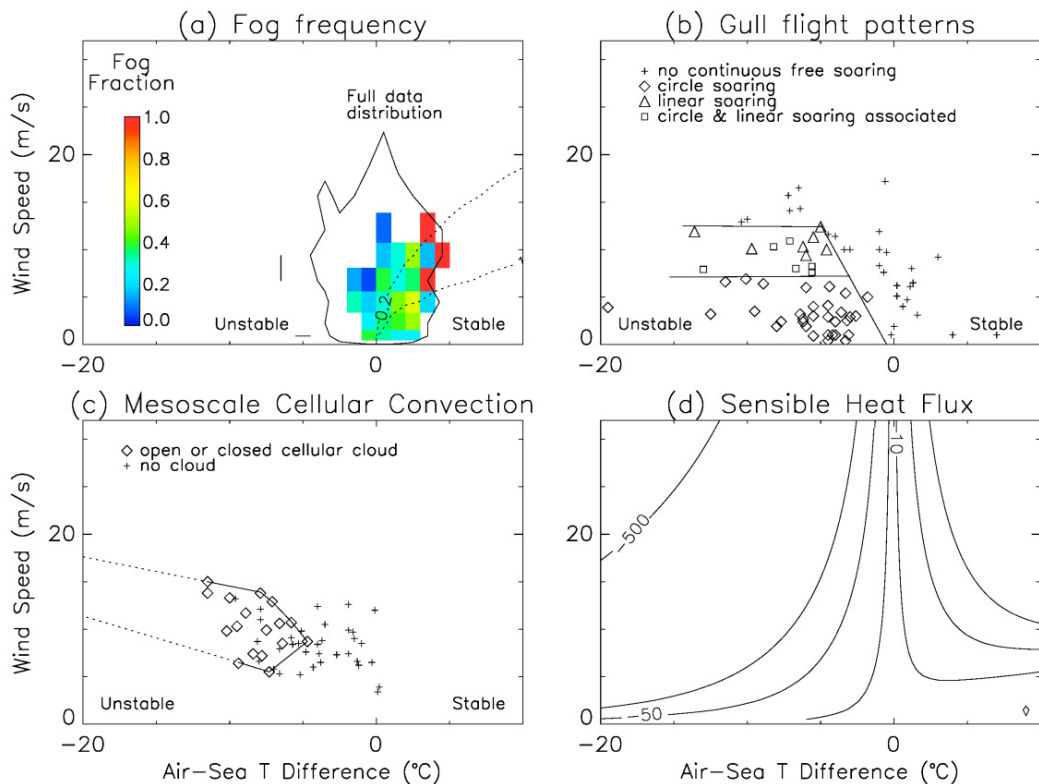

Fig.1. (a) The range of met-ocean measurements (solid black outline) and fraction of fog (color scale) recorded during the 1913 research cruise of the SS *Scotia* from Scotland to Newfoundland and Labrador [5,6]. The critical bulk Richardson number range for the onset of mechanical mixing (0.2–1.0) is shown by dotted lines and has been calculated for an air temperature of 10°C and a fog layer height of 200m. (b) Herring gull flight patterns recorded from a series of cruises in the subtropical western Atlantic Ocean [13]. In unstable atmospheric conditions, the gulls have a circular flight pattern in low winds and a linear soaring pattern in high winds. (c) Presence and absence of mesoscale cellular convective (MCC) clouds during the Air Mass Transformation Experiment in the East China Sea Feb.-Mar., 1975 [20,21]. (d) Sensible heat flux (in W/m^2) from a bulk turbulent heat flux algorithm based on Monin-Obukhov similarity theory [23].

observations were rare. The Woodcock diagram (as it was named by Grossman, 1982 [17]) was used to illustrate other boundary layer properties in subsequent decades, and its significance is reviewed by Garstang and Fitzgerald (1999) [18]. Woodcock (1975) [14] made minor revisions of the first studies from the 1940s that included a larger amount of data and also an unexpected static stability feature with significance for sea bird behavioural ecology.

2.3. Mesoscale Cellular Convection (MCC)

The organization of banded cloud structures ('Cloudstreets') over the ocean was described in an observational paper by Kuettner (1959) [19] who used the earlier observations of Woodcock to establish a link with the flux of heat and water vapor at the sea surface. Although banded cloud structures are a common occurrence over the ocean, they are also associated with extreme weather events, such the banded cloud formation surrounding hurricane centers. They are therefore an important element of understanding the wind structure of storms at sea. Sheu and Agee (1977) [20] and Agee and Sheu (1978) [21] presented information of mesoscale cellular convection (MCC) associated with cold air outbreaks over the East China Sea during the Air Mass Transformation Experiment (AMTEX) between Feb.-Mar., 1975. The main results of the project were framed with a U-ΔT diagram, shown in Fig. 1c for the daily average MCC clouds from Sheu and Agee (1977) [20]. The diagram highlights that the appearance of convective clouds over the ocean is a special feature of the unstable marine atmospheric boundary layer that occurs only at certain wind speeds. Sheu and Agee (1977) [20] related cloud structures to the surface fluxes of heat and moisture, and Agee and Sheu (1978) [21] underlined similarity between the MCC results and gull flight patterns of Woodcock (1940). The issue of understanding the met-ocean conditions that give rise to convective clouds is important for offshore wind energy in northwest Europe where severe autumn and winter storms are often associated with cold air outbreaks and a characteristic banded cloud structure [22].

2.4. Turbulent fluxes of heat, water vapor, and momentum

Turbulent fluxes of heat, water vapour, and momentum are typically parameterized with bulk formula incorporating the product of wind speed and a vertical property gradient in the atmosphere: temperature, water vapour mixing ratio, or wind speed. The vertical transport also depends on atmospheric stability, with unstable conditions leading to enhanced vertical transport through the atmosphere. Because bulk parameterizations of sensible heat flux depend on the product of air-sea temperature difference and wind speed, they can be readily illustrated with the U-ΔT diagram. Fig. 1d shows the sensible heat flux from Smith (1988) [23] on U-ΔT axes (i.e., calculated assuming a typical value of 75% relative humidity over the ocean). The left-right asymmetry in the diagram across the 0°C temperature line results from the different vertical profile correction functions used for stable and unstable conditions, and these parameterize the enhanced vertical mixing effects in unstable convective conditions. Smith (1988) [23] makes a series the tabulations of heat and momentum transfer coefficients in the format of a U-ΔT table. These represent a summary of the state of understanding of surface heat fluxes on the basis of Monin-Obukhov theory for a limited set of observations at moderate wind speeds. However, for wind speeds >25m/s there are few direct flux measurements, and the available information indicates that surface turbulent fluxes may be significantly modified by sea spray, roll vortices, and large waves.

2.5. Air Pollutant Dispersion

The dispersion of air pollutant clouds near the sea surface depends on conditions of atmospheric stability and wind speed and can be analysed with the U-ΔT diagram. Early research on tracer dispersion problems were conducted near the end World War II in the context of naval smoke screens, and the stability of the marine atmospheric boundary layer was recognized to be an important factor [24]. Prophet (1961) [25] made a literature review of the marine atmospheric boundary layer for the U.S. Army Chemical Corp Meteorological Program that focused on meteorological factors on dose levels associated with near surface pollutant clouds. The report was produced during a period in the Cold War when issues of aerosol pesticides and radioactive clouds from weapons tests and nuclear reactor accidents were important. In following decades, the need to understand accidental radiation releases from coastal nuclear reactors motivated a series of coastal experiments in New York [26], California [27], and in the Oresund Strait between Sweden and Denmark [28]. The theoretical understanding of tracer cloud dispersion in the

marine atmosphere grew out of research initiated by Taylor (1915) [7] on the vertical diffusion of heat and water vapour in the marine atmospheric boundary layer and by Pasquill (1961) [29] on the meteorological thresholds to assess industrial air pollution over land. For the marine atmospheric boundary layer, these approaches were unified within the context of Monin-Obukhov length scales [27,30,31]. Fig. 2a shows a U-ΔT diagram with Monin-Obukhov lengths scales for tracer dispersion analysis, and is similar to the diagram of Hsu (1992) [31]. In this diagram, neutral atmospheric stability conditions are defined between Monin-Obukhov length scales of -25m to +25m, with unstable conditions in the region -25m to -5m and stable conditions in the region +25m to +5m. In general, stable conditions lead to tracer clouds being concentrated near the surface, while neutral and unstable conditions facilitate the vertical dispersal of pollutants.

2.6. White cap formation

Investigations of whitecaps on the ocean started within the context of operational ocean wave studies soon after World War II [32]. Whitecap studies intensified from the late 1960s because of the impact of foam on brightness temperature recorded by airborne and satellite passive radar sensors that provided a way to retrieve surface wind speeds from space [33]. Additionally, whitecaps are important in atmospheric chemistry because of the link between whitecap cover and sea salt aerosol production and oceanic outgassing [34,35]. Munk (1947) [32] pointed
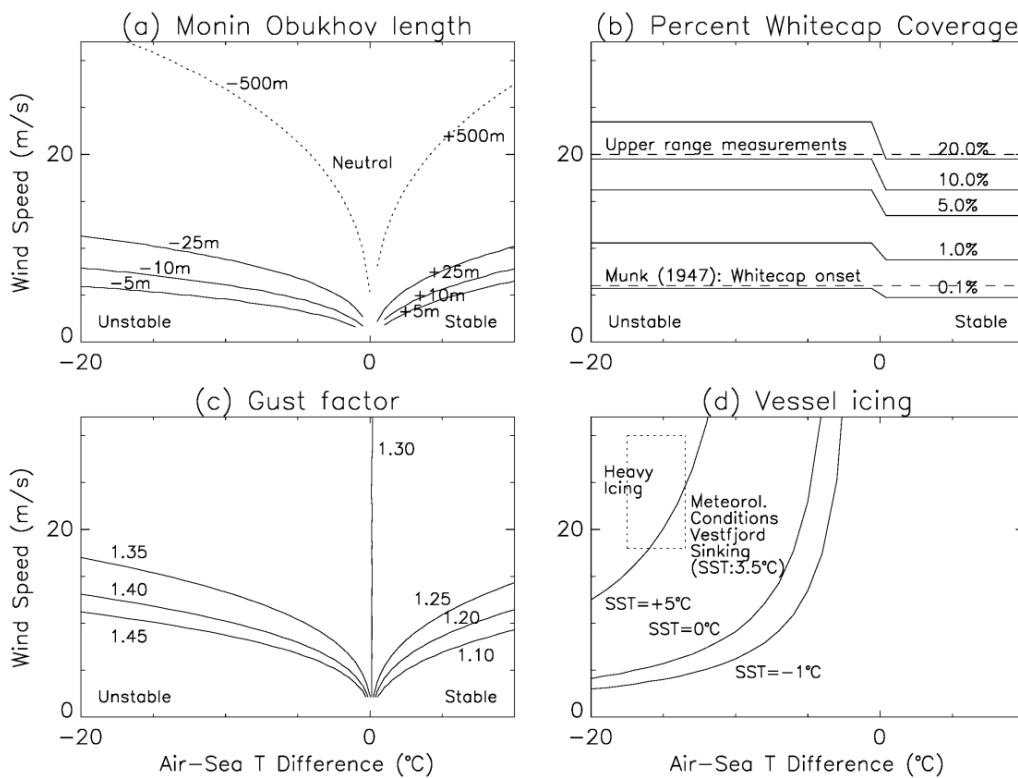

Fig.2. (a) Monin-Obukhov length calculated from the flux parameterization of Smith (1988) [23] assuming a typical MABL relative humidity of 75%. (b) Percent whitecap coverage showing hypothesized atmospheric stability dependence [37]. The dashed lines give the onset threshold for whitecap formation hypothesized in the early study of Munk (1947) [32] and the upper range of available measurements of Monahan (1971) [36]. (c) Parameterized gust factor dependence on Monin-Obukhov length. (d) Threshold lines for onset of heavy superstructure icing for three values of sea surface temperature. Met-ocean conditions for the 1989 sinking of the trawler *Vestfjord* in the Gulf of Alaska are shown by the dashed box [43]. The sea surface temperature at the time of the sinking was 3.5°C, and there was large uncertainty in the reported wind speeds at the time of the accident.

out a critical threshold of wind speed before oceanic whitecaps started to form. Subsequent investigations of whitecaps using photographic interpretation did not support the critical threshold hypothesis but instead linked oceanic whitecap coverage to wind speed through a power law relationship [36]. Modern investigations of the relation between significant wave height and wind speed indicate a greater tendency for higher waves (and perhaps whitecap formation) in unstable atmospheric conditions. However, early investigations suggested the converse relationship and higher whitecap coverage for stable atmospheric conditions [37]. Modern assessments of the problem point out that the early investigations had been based on image interpretation of a limited number of photographs that did not span the full parameter space defined by wind speed, air temperature, and sea surface temperature [38]. Whitecap formation depends on sea surface temperature and salinity so that the physical and rheological properties of seawater are important. Fig. 2b shows a U-ΔT diagram of whitecap coverage that summarizes the stability-dependent power law relationships and threshold approach of Wu (1979) [37].

2.7. Gust factors and turbulence intensity

Wind loading of offshore structures is an important concern in the oil/gas industry and also for offshore wind energy [39]. The wind loading encompasses of the effects of gusts during hurricanes, but it also relates to the effects of cumulative fatigue from turbulence at lower wind speeds, and this is important for maintenance issues of offshore
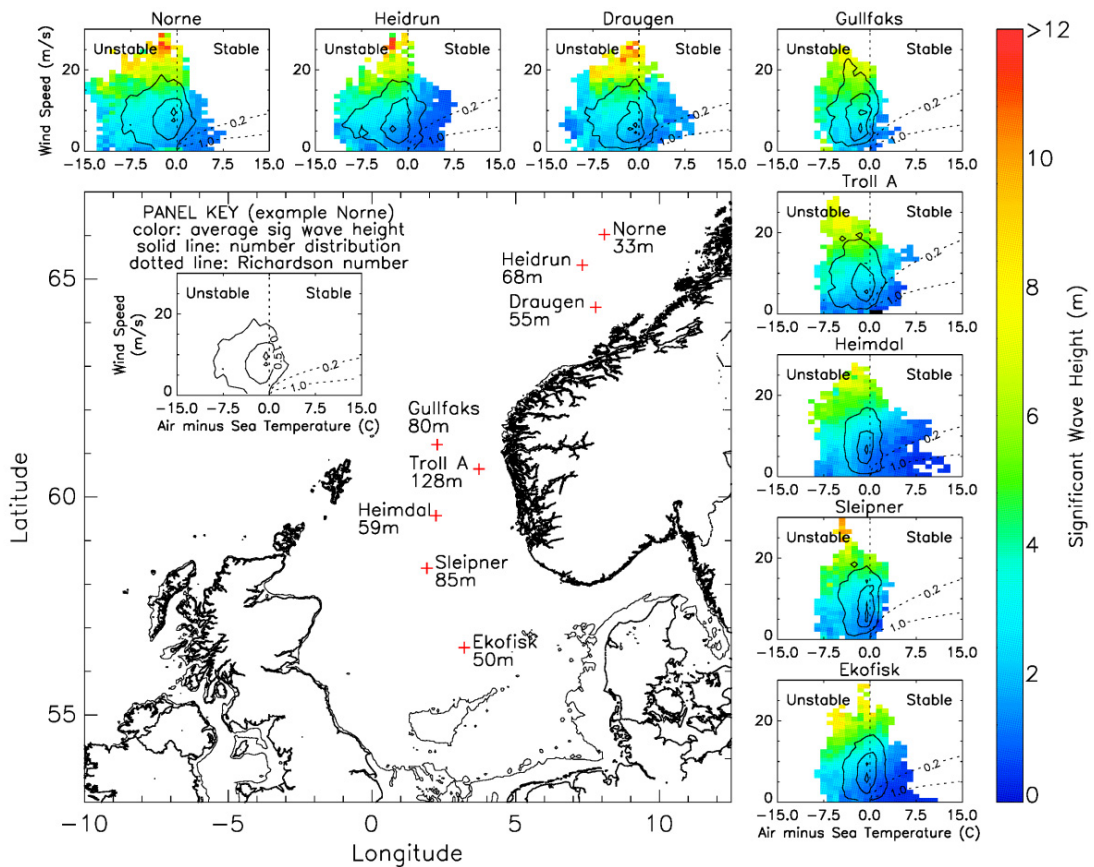

Fig.3. Average significant wave height (colour field) on U-ΔT axes for eight Norwegian offshore oil platforms. The wave height statistics have been evaluated with wind speed bins of 1m/s and temperature difference bins of 1°C. The joint probability distribution for each platform is plotted on the U-ΔT axes with solid lines. Dotted lines show the approximate bulk Richardson numbers (calculated for the platform instrument height and an assumed air temperature of 10°C) of 0.2 and 1.0 for the onset of mechanical mixing in stable atmospheric conditions. The map of northwest Europe shows the location of the platforms and the meteorological instrument heights from the Eklima database.

wind turbines [11]. For offshore buoys of the National Buoy Data Center, maximum gusts are calculated based on a 5s average of an 8 minute wind speed record, and the gust factor is the ratio of the maximum gust to the average wind speed. Turbulence intensity, a diagnostic quantity of particular importance for offshore wind energy, is calculated as the standard deviation divided by average of the wind speed. Hsu (2003a) [40] links gust factor and turbulence intensity with Monin-Obukhov similarity theory, and these diagnostics can be plotted on a U-ΔT diagram, as shown in Fig.2c. The diagram highlights that gust factors increase from stable to unstable conditions. High frequency sonic measurements of wind speed from the FINO1 mast in the North Sea indicate that the actual relationship of measured turbulence intensity over the North Sea may be more complicated than indicated in Fig.2c [41]. Possibly, Monin-Obukhov similarity theory may break down at high wind speeds greater than 20m/s when the marine atmospheric boundary layer is characterized by propagating roll vortices that extend at least to several hundred meters height. The nature of wind loading of offshore structures in storms is an important problem in operational meteorology.

2.8. Superstructure Icing

A series of rapid vessel sinkings in the 1960-1980s led to a series of programs to understand the phenomenon superstructure ice formation [42,43]. The accidents had been associated with an expansion and maritime activities and particularly fishing in high northern latitudes. Superstructure icing from sea spray at subfreezing temperatures
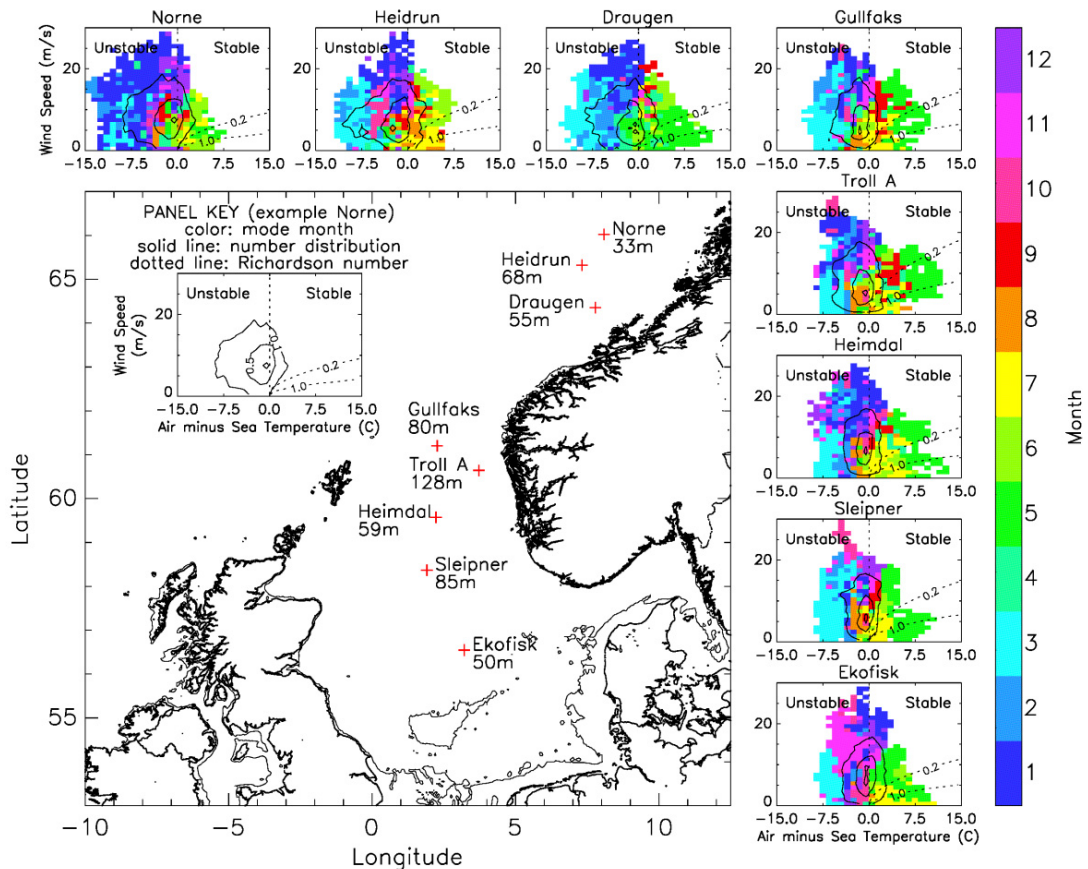

Fig. 4. As for Fig.3 but showing modal month of the data distribution within each bin of the U-ΔT field. For this time segment 2005–2007, the worst storms for the Norwegian Sea platforms are mostly in January, while the North Sea has a predominance of severe storms in October and November.

was found to be a serious threat to small offshore fishing vessels, owing to the low vessel freeboard and similarity between the vessel length and dominant wavelength during storms. The vessel losses mostly occurred during storms that were associated with cold air outbreaks in the North Pacific, North Atlantic, and Arctic Oceans. Quantitative datasets of superstructure were difficult to assess and quality check because of the additional importance of ship size and heading with respect to the ambient wave field. Among the met-ocean parameters, wind speed, air temperature, and sea temperature were highlighted to be the most important geophysical factors that determined the rate of superstructure ice accumulation. Summarizing empirical data, early investigators explored a number of graphical presentation formats to show the multi-dimensional datasets [44]. The analysis of Overland (1990) [43] appeared late in the research period and was regarded as the most accurate because of its tests on data sets from the Pacific and Atlantic Oceans. Overland (1990) [43] presented rates of superstructure icing on axes of wind speed versus air temperature for different sea surface temperatures, but the major issues are also illustrated on U-ΔT axis. Fig.2d shows a summary of icing information on U-ΔT axis, showing thresholds heavy icing (i.e., >2cm/hour of ice accumulation; a serious threat to vessel safety) for three different sea surface temperatures: -1°C, 0°C, and 5°C. While dangerous ice build-up is a serious issue at low sea temperatures below ~2°C, cases of superstructure icing have been documented at sea temperatures over 6°C for very low air temperatures and high wind speeds. Fig.2d illustrates the met-ocean conditions for the case of the sinking of the trawler *Vestfjord* in the Gulf of Alaska in 1989 [43], and it highlights the importance of the diagram for operational icing forecasts [44]. The issue of the icing of offshore structures is still an issue as offshore oil/gas development advances into Arctic regions [45] and wind farms are constructed in cold maritime climates.

3. The U-ΔT Diagram for Met-Ocean Conditions at Norwegian Offshore Platforms

The development of offshore oil in Europe drove the need to understand wind speed and atmospheric turbulence characteristics in the North Sea and Norwegian Sea [46,47]. Eidsvik (1985) [46] analyzed a high frequency data set collected at a 110m derrick on the Statfjord A platform between June, 1979 and Apr., 1982. Andersen and Løvseth (1995) [47] reported on the analysis of high frequency data collected at a series of high meteorological masts between Feb., 1988 and May, 1989 at a coastal location at Frøya near Trondheim in mid-Norway. In both cases, the U-ΔT diagram was an important component of the initial data survey to understand the wind speed distribution as a function of atmospheric stability. These are reviewed by Kettle (2014b) [41] along with corresponding information from FINO1 in the North Sea, an offshore meteorological mast that was set up to support the development of German offshore wind farms.

The availability of recent met-ocean data from a series of Norwegian offshore platforms in the Norwegian Sea and North Sea presents an opportunity to extend the U-ΔT analysis to cover a larger ocean area. The met-ocean information in the Eklima database includes measured meteorological and wave information for the platforms Draugen, Norne, and Heidrun in the Norwegian Sea and Troll A, Gullfaks, Sleipner A, Heimdal, Ekofisk in the North Sea. Like many offshore datasets, the measurement conditions are not perfect. The meteorological measurements may be affected by flow distortion around the platforms [48]. The original high frequency meteorological data are not available for spectral analysis, and the Eklima database presents 20 minute averages. There are data gaps in certain time series, and the platforms Troll A, Gullfaks, Sleipner A, and Heidrun have no in situ sea surface temperature information in the chosen three year investigation period of 2005–2007. This was overcome by use of data from the European Space Agency Sea Surface Temperature Climate Change Initiative (ESA SST CCI) for the year 2006. The present analysis focuses on significant wave height, which is important for understanding wave loads on offshore structures, and also considers the date stamp information of the met-ocean data to draw conclusions about the seasonality of strong storms.

The results of average significant wave height on U-ΔT axes are shown for the eight Norwegian platforms in Fig.3 along with a map of the platform location off northwest Europe. The joint probability distributions show a wide range of the atmospheric stability conditions ranging from approximately -15°C to +10°C and average wind speeds range up to 30m/s, which is near the hurricane threshold. The strongest winds occur at slightly unstable atmospheric conditions. The data distribution is asymmetrically distributed between stable and unstable atmospheric conditions. Unstable conditions predominate for the Norwegian Sea platforms, with cases of air minus sea temperatures extending to -15°C, and this may indicate a tendency toward cold air outbreaks in proximity to

edge of sea ice in winter. The highest significant wave heights are associated with the highest wind speeds at mostly unstable atmospheric conditions. For stable atmospheric conditions, significant wave heights tend to be lower, and this is likely associated with an atmospheric decoupling effect near the sea surface.

The modal month distribution from the original time series data is shown on U-ΔT axes in Fig.4. The diagram is important in documenting seasons where storms and calm periods are expected at the different platforms. The seasonal patterns are different between the platforms in the Norwegian Sea and the North Sea. The North Sea platforms have a high proportion of the most severe wind storms in October and November, while the Norwegian Sea stations have a greater tendency of the most severe wind storms in January. Calm, stable conditions predominate in May, June, and July.

4. Conclusion

A review of the U-ΔT format for met-ocean data presentation highlights important features of offshore meteorological research through the 20th century. A number of important concepts for operational meteorology are linked through the U-ΔT axes: fog incidence, cellular convection and roll vortices, mesoscale convective clouds, surface heat fluxes, whitecap formation, and superstructure icing conditions. An analysis of the recent met-ocean data sets from the Norwegian offshore oil platforms shows a set of features that are mostly consistent with earlier studies, although the platform data spans a greater parameter range. For significant wave height, the U-ΔT diagrams indicate that the largest waves occur during unstable atmospheric conditions and high winds. An analysis of the monthly modes of data distribution on U-ΔT axes reveals that severe late autumn storms predominate in the North Sea, while the worst storms Norwegian Sea are most frequent in January. Offshore wind turbines are sensitive to ambient turbulence conditions for long periods of operation without maintenance. The large spread of atmospheric stability conditions at the northern Norwegian platforms may indicate less ideal conditions for offshore wind farms. This review highlights a number of unresolved issues of operational meteorology. For offshore wind energy, the most important issues may be the structure of internal boundary layers and atmospheric dynamics during storms.

References

[1] Bilgili M, Yasar A, Simsek E. Offshore wind power development in Europe and its comparison with onshore counterpart. Renewable and Sustainable Energy Reviews 2011;15:905-915.
[2] Sun X, Huang D, Wu G. The current state of offshore wind energy technology development. Energy 2012;41:298-312.
[3] Sorensen T, Jensen V, Raben N, Lykkegaard J, Saxov J. Lightning protection for offshore wind turbines. CIRED, 18-21 June, 2001, Conference publication No. 482, IEE; 2001.
[4] Quarton, D.C., An international design standard for offshore wind turbines: IEC 61400-3, http://wind.nrel.gov/public/SeaCon/Proceedings/Copenhagen.Offshore.Wind.2005/documents/papers/Design_basis/D.Quarton_An_internat ional_design_standard_for_offshore.pdf, 2005.
[5] Taylor GI. Report of the work carried out by the SS 'Scotia', 1913, Report to the Board of Trade, London; 1914.
[6] Taylor GI. The formation of fog and mist. Q J R Meteorol Soc 1917;43:241-263.
[7] Taylor GI. Eddy motion in the atmosphere. Phil Trans R Soc Lond A 1915;215:1-26.
[8] Garratt JR. The internal boundary layer – a review. Bound-Layer Meteorol 1990;50:171-203.
[9] Sathe A, Gryning SE, Peña A. Comparison of the atmospheric stability and wind profiles at two wind farm sites over a long marine fetch in the North Sea. Wind Energy 2011;14:767-780.
[10] Argyle P, Watson SJ. Assessing the dependence of surface layer atmospheric stability on measurement height at offshore locations. J Wind Eng Ind Aerodyn 2014;131:88-99.
[11] Kettle AJ. Unexpected vertical wind speed profiles in the boundary layer over the southern North Sea. J Wind Eng Ind Aerodyn 2014;134:149-162.

[12] Woodcock AH. Convection and soaring order the open sea. J Mar Res 1940;3:248-253.
[13] Woodcock AH. Soaring over the open sea. The Scientific Monthly 1942;55:226-232.
[14] Woodcock AH. Thermals over the ocean and gull flight behaviour. Bound-Layer Meteorol 1975; 9:63-68.
[15] Priestley CHB. Convection from the earth's surface. Quart J Roy Meteorol Soc 1955;81:139-143.
[16] Deardorff JW. Discussion of 'thermals over the sea and gull flight behavior' by A.H. Woodcock. Bound-Layer Meteorol 1976;10:241-246.
[17] Grossman RL. An analysis of vertical velocity spectra obtained in the BOMEX fair-weather, trade-wind boundary layer. Bound-Layer Meteorol 1982;23:323-357.
[18] Garstang M, Fitzgerald DR. Observations of surface to atmosphere interactions in the tropics. Oxford University Press; 1999.
[19] Kuettner J. The band structure of the atmosphere. Tellus 1959;11:267-294.
[20] Sheu PJ, Agee EM. Kinematic analysis and air-sea heat flux associated with mesoscale cellular convection during AMTEX 75. J Atmos Sci 1977;34:793-801.
[21] Agee EM, Sheu PJ. MCC and gull flight behaviour. Bound-Layer Meteorol 1978;14:247-251.
[22] Vincent CL, Hahmann AN. Hour-scale wind fluctuations over the North Sea. EWEA Annual Event 2011, Brussels, Belgium, 14-17 March; 2011.
[23] Smith SD. Coefficients for sea surface wind stress, heat flux, and wind profiles as a function of wind speed and temperature. J Geophys Res 1988;93:15467-15472.
[24] Woodcock AH, Wyman J. Convective motion in the air over the sea. Ann N Y Acad Sci 1947;68:749-777.
[25] Prophet DT. Survey of the available information pertaining to the transport and diffusion of airborne material over ocean and shoreline complexes. Technical Report No. 89, Aerosol Laboratory, Stanford University, Stanford, California, US Army Chemical Corps, Research and Development Contract, DA-48-007-403-CML 448; June, 1961.
[26] Raynor GS, Michael P, Brown RM, Sethuraman S. Studies of atmospheric diffusion from a nearshore oceanic site. J Appl Meteorol 1975;14:1080-1094.
[27] Schacher GE, Fairall CW, Zanetti P. Comparison of stability classification methods for parameterizing coastal overwater dispersion. Proceedings, First International Conference on Meteorology and Air/Sea Interaction of the Coastal Zone, The Hague, Netherlands; May 10-14, 1982. p 77-82.
[28] Melas D. The temperature structure in a stably stratified internal boundary layer over a cold sea. Bound-Layer Meteorol 1989;48:361-375.
[29] Pasquill F. The estimation of the dispersion of windborne material. Meteorological Magazine 1961;90:33-49.
[30] Hasse L, Weber H. On the conversion of Pasquill categories for use over sea. Bound-Layer Meteorol 1985;31:177-185.
[31] Hsu SA. An overwater stability criterion for the offshore and coastal dispersion model. Bound-Layer Meteorol 1992;60:397-402.
[32] Munk WH. A critical wind speed for air-sea boundary processes. J Mar Res 1947;6:203-218.
[33] Ross DB, Cardone V. Observations of oceanic whitecaps and their relation to remote measurements of surface wind speed. J Geophys Res 1974;79:444-452.
[34] Monahan EC. Oceanic whitecaps: sea surface features detectable via satellite that are indicators of the magnitude of the air-sea gas transfer coefficient. Proc Indian Acad Sci (Earth Planet Sci) 2002;111:315-319.
[35] Lewis ER, Schwartz SE. Sea salt aerosol production: Mechanisms, methods, measurements and models – a critical review. American Geophysical Union; 2004.
[36] Monahan EC. Oceanic whitecaps. J Phys Oceanogr 1971;1:139-144.
[37] Wu J. Oceanic whitecaps and sea state. J Phys Oceanogr 1979;9:1064-1068.
[38] Babanin A. Breaking and dissipation of ocean surface waves. Cambridge University Press; 2011.
[39] Hsu SA. Estimating overwater friction velocity and exponent of power-law wind profile from gust factor during storms. Journal of Waterway, Port, Coastal, and Ocean Engineering 2003;July/August:174-177.
[40] Hsu SA. A gust-factor criterion for rapid determination of atmospheric stability and mixing height for overwater dispersion estimates. National Weather Digest 2003;27:70-74.
[41] Kettle AJ. A diagnostic diagram to understand atmosphere-ocean dynamics in the southern North Sea at high wind speeds. (European Geosciences Union General Assembly 2014, EGU 2014). Energy Procedia 2014;59:1-8.
[42] Panov VV. Icing of ships. Polar Geography 1978;2:166-186.
[43] Overland JE. Prediction of vessel icing for near-freezing sea temperatures. Weather and Forecasting 1990;5:62-77.
[44] Feit DM. Forecasting of superstructure icing for Alaskan waters. Marine 1987;12:5-10.
[45] Efimov YO. Vessel icing on the Shtokman FPSO. M Sc thesis. University of Stavanger; June 25, 2012.
[46] Eidsvik KJ. Large-sample estimates of wind fluctuations over the ocean. Bound-Layer Meteorol 1985;32:103-132.
[47] Andersen OJ, Løvseth J. Gale force marine wind. The Frøya data base. Part 1: Sites and instrumentation. Review of the data base. J Wind Eng Ind Aerodyn 1995;57:97-109.
[48] Berge E, Byrkjedal O, Ydersbond Y, Kindler D. Modelling of offshore wind resources. Comparison of mesoscale model and measurements from FINO1 and North Sea oil rigs. Proceedings of EWEC2009 Marseille; March 2009.